

# DNA Binding Properties of 2,7-Diazapyrene and Its *N*-Methylated Cations Studied by Linear and Circular Dichroism Spectroscopy and Calorimetry

Hans-Christian Becker\* and Bengt Nordén\*

Contribution from the Department of Physical Chemistry, Chalmers University of Technology, S-412 96 Göteborg, Sweden

Received November 12, 1996<sup>⊗</sup>

**Abstract:** The binding of 2,7-diazapyrene (DAP), *N*-methyl-2,7-diazapyrenium monocation (MDAP), and *N,N'*-dimethyl-2,7-diazapyrenium dication (DMDAP) to calf thymus DNA has been studied with respect to molecular geometry and thermodynamics. It is concluded from flow linear dichroism (LD) and induced circular dichroism (CD) spectra that the three diazapyrenes bind by intercalation to alternating AT as well as GC polynucleotide duplexes, as indicated by strong interactions with the transitions of the nucleobases in conjunction with approximately perpendicular orientations of the in-plane symmetry axes relative to the DNA helix axis. The reduced LD ( $LD^r = LD/A_{180}$ ) of the DNA complexes is characterized by marked fine structure, decreasing in the order DAP > MDAP > DMDAP. This finding is interpreted in terms of a microscopic heterogeneity associated with rotational mobility of the ligand in a tilted intercalation pocket, with the dication DMDAP having less rotational freedom than the neutral DAP has. Other distinct differences between the three diazapyrenes are revealed in their thermodynamic parameters of binding. DAP binds with a negative  $\Delta H^\circ$  ( $-9$  kcal/mol) and a negative  $\Delta S^\circ$  ( $-7$  cal/(mol K)), whereas the binding of the dication DMDAP is entropically driven ( $+43$  cal/(mol K)) but enthalpically disfavored ( $+5.2$  kcal/mol), the monocation MDAP having an intermediate position ( $\Delta H^\circ = -3$  kcal/mol,  $\Delta S^\circ = +12$  cal/(mol K)).

## Introduction

To gain insight into the nature of interactions and binding geometry of aza-aromatic compounds with DNA, we have conducted a spectroscopic and calorimetric study of 2,7-diazapyrene (DAP) and its two cationic homologues *N*-methyl-2,7-diazapyrenium monocation (MDAP) and *N,N'*-dimethyl-2,7-diazapyrenium dication (DMDAP) (Figure 1). The parent compound DAP has been the subject of both spectroscopic<sup>1–3</sup> and electrochemical<sup>4–6</sup> investigations, and its electronic properties are well understood. The DNA interactions with DMDAP have previously been studied in electron-transfer<sup>7–9</sup> and photocleavage<sup>10</sup> experiments.

In the series of diazapyrenes DAP, MDAP, and DMDAP, major variations in ground-state properties are due to changes in charge and dipole moments and hydrogen bonding capabilities. The excited states properties parallel those of the ground state with respect to energies and orbital symmetries, thus facilitating assessment of DNA binding geometries by polarized-light spectroscopy. The 2,7-diazapyrene chromophore provides a unique structural probe for which flow linear dichroism (flow LD) is ideal for analyzing binding geometries of its nucleic acid

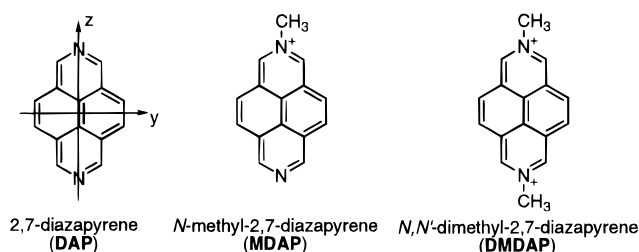


**Figure 1.** Structural formulas of the diazapyrenes with internal coordinate axes.

complexes.<sup>11</sup> The first two  $\pi-\pi^*$  transitions, polarized along the in-plane symmetry axes *y* and *z* as shown for DAP (Figure 1), are spectrally well resolved and thereby allow the orientations of these axes relative to DNA to be determined. Finally, thermodynamic data for the DNA interaction of the diazapyrenes obtained from calorimetric and equilibrium measurements are used to assess the respective contributions to binding affinity by hydrogen bonding and electrostatic and hydrophobic effects.

## Materials and Methods

**Reagents and Solvents.** - DAP, MDAP, and DMDAP were prepared according to the literature.<sup>6,7</sup> Calf thymus DNA (CT DNA; Sigma), homopolynucleotides poly(dA-dT)·poly(dA-dT) (AT; Pharmacia Biotech), and poly(dG-dC)·poly(dG-dC) (GC; Aldrich) were used as obtained. Unless stated otherwise, aqueous solutions were 10 mM in NaCl and 1 mM in cacodylate buffer (pH 7). Water resistivity was  $>10$  M $\Omega$ /cm.

**Spectroscopy.** Absorption spectra were recorded on Kontron Uvikon 810, Cary 2300, and Cary 4B spectrometers and fluorescence spectra on a SPEX Fluorolog  $\tau$ -2 instrument. Lifetime measurements were performed on the SPEX (using the phase-modulation technique) and on an Edinburgh single-photon counting instrument with a Jobin–Yvon monochromator in the emission channel. Aqueous solutions of

<sup>⊗</sup> Abstract published in *Advance ACS Abstracts*, June 1, 1997.

(1) Thulstrup, E. W.; Downing, J. W.; Michl, J. *Chem. Phys.* **1977**, *23*, 307–319.

(2) Thulstrup, E. W.; Michl, J. *J. Am. Chem. Soc.* **1982**, *104*, 5594–5604.

(3) Bruhin, J.; Gerson, F. *Helv. Chim. Acta* **1975**, *58*, 2422–2431.

(4) Hünig, S.; Gross, J. *Tetrahedron Lett.* **1968**, 2599–2604.

(5) Hünig, S.; Gross, J. *Tetrahedron Lett.* **1968**, 4139.

(6) Hünig, S.; Gross, J.; Lier, E. F.; Quast, H. *Liebigs Ann. Chem.* **1973**, 339–358.

(7) Blacker, A. J.; Jazwinski, J.; Lehn, J.-M. *Helv. Chim. Acta* **1987**, *70*, 1–12.

(8) Brun, A. M.; Harriman, A. *J. Am. Chem. Soc.* **1991**, *113*, 8153–8159.

(9) Brun, A. M.; Harriman, A. *J. Am. Chem. Soc.* **1992**, *114*, 3656–3660.

(10) Blacker, A. J.; Jazwinski, J.; Lehn, J.-M.; Wilhelm, F. X. *J. Chem. Soc., Chem. Commun.* **1986**, 1025–1037.

(11) Nordén, B. *Appl. Spectrosc. Rev.* **1978**, *14*, 157–248.

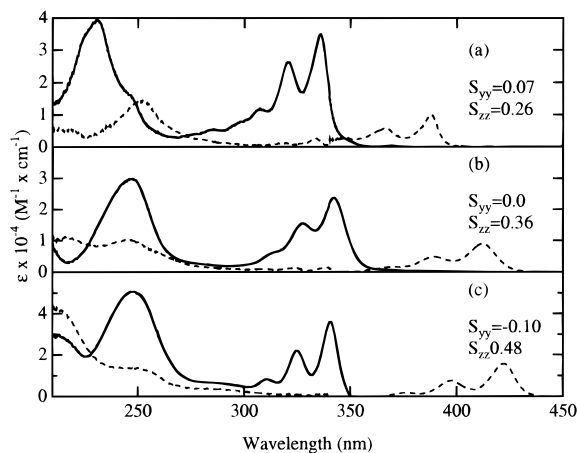


**Figure 2.** Polarized resolved electronic absorption spectra of (a) DAP, (b) MDAP, and (c) DMDAP obtained from LD spectra in stretched PVA (see Materials and Methods, the orientation parameters applied to resolve the spectra are given in the respective panels). Solid line spectra represent transitions polarized along the molecular long axis ( $z$ ), and dashed line the short axis ( $y$ ) of the diazapyrene moiety. Practically pure  $y$  polarizations are noted at 390 nm (DAP), 410 nm (MDAP), and 420 nm (DMDAP) and  $z$  polarizations at 310–340 nm, in all three compounds.

the pure diazapyrenes followed Lambert–Beer’s law in the relevant concentration region used.

Flow linear dichroism was measured on a Jasco J-500A circular dichroism spectrometer, equipped with an Oxley prism for LD operation. The reduced dichroism was calculated as  $LD^r = LD/A_{iso} = (A_{||} - A_{\perp})/(\text{normal absorbance spectrum})$ .<sup>11,12</sup> Circular dichroism was measured on a Jasco J-720 spectropolarimeter. Stretched film measurements were made in poly(vinyl alcohol) films.<sup>11–13</sup> The linear dichroism was calculated as  $A_{||} - A_{\perp}$  and the  $LD^r$  for film spectra as  $LD/(A_{||} + 2A_{\perp})$ . Since the long- and short-axis polarized transitions are energetically well-separated, the orientation parameters and resolved spectra can be obtained through a linear combination of LD and  $A_{iso}$ .<sup>11,13</sup> The resolved spectra,  $A_z$  and  $A_y$ , corresponding to polarizations parallel to the long and short in-plane axes, respectively, are related to the measured LD according to<sup>11–13</sup>

$$LD = A_{||} - A_{\perp} = S_{zz}A_z + S_{yy}A_y + S_{xx}A_x \quad (1)$$

where  $S_{ij}$  are the orientation parameters for the respective molecular axes. The resolution is based on the assumption of negligible out-of-plane polarized intensity ( $A_x = 0$ ).

**Calorimetry.** Isothermal titration calorimetry was carried out on a Microcal ITC instrument. The same buffers and ionic strengths were used as in the spectroscopic measurements. Baseline corrections were small and performed automatically. Control experiments carried out by titrating buffer into buffer, ligand into buffer, and buffer into DNA showed that heats of dilution were negligible. The titrations were analyzed by the one- and two-site models supplied with the Microcal software.

## Results

**Electronic Absorption Spectra.** The absorption spectra of DAP, MDAP, and DMDAP resemble the spectrum of pyrene in terms of vibrational structure and band assignments (Figure 2), the band at  $>350$  nm corresponding to the forbidden  $L_b$  transition.<sup>1,2</sup> Upon  $N$ -methylation, the difference in extinction coefficients between the  $L_b$  and  $L_a$  transitions of DAP around 400 and 330 nm, respectively, decreases, while the absorption intensity in the 200–300 nm region increases significantly. Stretched film measurements (Figure 2) confirm the  $L_b$  and  $L_a$

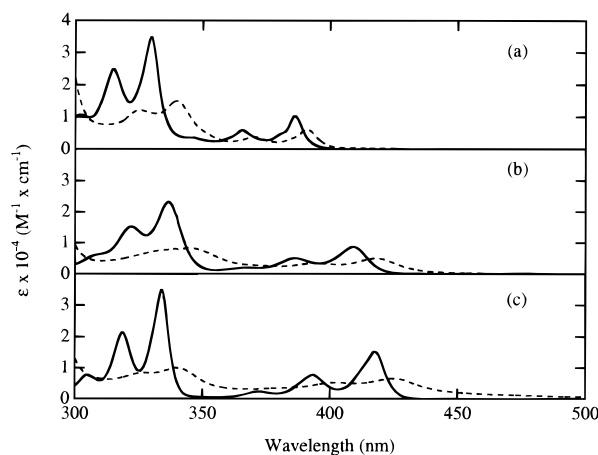


**Figure 3.** Absorption spectra of the diazapyrenes, free (solid lines) and bound to DNA (dotted lines): (a) DAP, (b) MDAP, (c) DMDAP.

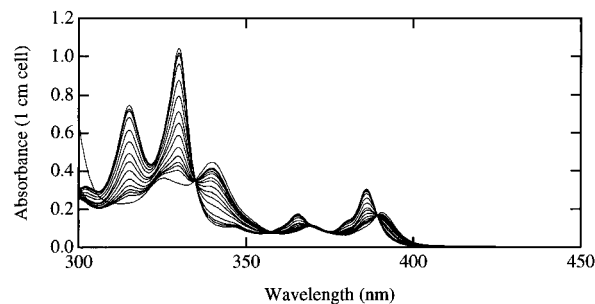


**Figure 4.** Example of absorbance titration of DAP with DNA. Note the four isosbestic points.

transition moments to be purely polarized along the in-plane molecular short and long axes, respectively. The absorption spectra of the protonated forms of DAP,  $HDAP^+$ , and  $H_2DAP^{2+}$ , observed in acidic solutions of DAP, are similar to those of MDAP and DMDAP, respectively.

**Spectral Effects Upon Addition of DNA.** The spectral changes upon addition of CT DNA to solutions of DAP, MDAP, and DMDAP are characterized by hypochromicity (*ca.* 60%), accompanied by bathochromic shifts and broadening of the  $L_a$  and  $L_b$  absorption bands (Figure 3a–c). The onset of absorption of the DMDAP–DNA complex is markedly red-shifted which may be due a broad charge-transfer band. A similar, though less pronounced spectral feature is seen also for the MDAP–DNA complex but is absent in the absorption spectrum of the DAP–DNA complex. Complexation of DAP, MDAP, and DMDAP with DNA is completely reversible upon addition of sodium dodecyl sulfate, proving that binding does not involve formation of covalently bound adducts. Addition of homopoly-nucleotide duplexes AT and GC to solutions of DAP, MDAP, and DMDAP results within experimental error in the same spectral effects as described for CT DNA.

**Binding Constants.** Binding affinities of the diazapyrene–DNA complexes were assessed by absorbance titrations (Figure 4). Least-squares fits of the intermediate spectra to the start- and end-point spectra in the region 330–500 nm according to

$$A(\text{total}) = \alpha A(\text{free}) + \beta A(\text{bound}) \quad (2)$$

yielded the fractions of free and bound ligand. The sum of the coefficients ( $\alpha + \beta$ ) did not deviate significantly from unity. This is in line with the observation of several isosbestic points (Figure 4), indicating the presence of a single spectroscopically detectable bound species only. For the DNA case, a macroscopic model for the ligand binding was applied:

(12) Nordén, B.; Kubista, M.; Kurucsev, T. *Q. Rev. Biophys.* **1992**, *25*, 51–170.

(13) Thulstrup, E. W.; Michl, J. *Spectroscopy with Polarized Light. Solute Alignment by Photoselection, in Liquid Crystals, Polymers, and Membranes*; VCH Publishers: New York, 1995.

$$K = \frac{[SL]}{[L][S]} = \frac{[SL]}{\{[L_{\text{tot}}] - [SL]\}\{n[P_{\text{tot}}] - [SL]\}} \quad (3)$$

with  $K$  the effective stability constant,  $[L]$  the free ligand concentration,  $[P_{\text{tot}}]$  the total DNA concentration as phosphate, and  $[SL]$  the concentration of complex. The total concentration of binding sites is defined as  $n[P_{\text{tot}}]$ . Simplex optimization gave a good fit to the experimental data for the parameters summarized in Table 1. It was therefore not considered meaningful to use a more sophisticated binding model for the heterogeneous CT DNA.<sup>14,15</sup>

The binding constants for the association of DAP, MDAP, and DMDAP with AT and GC were determined by fluorescence titrations (Supporting Information, Figure A). The fluorescence intensity change was converted to concentration of free diazapyrene. With the exception of DAP-AT, which under certain conditions exhibits stronger fluorescence than free DAP, the polynucleotide–ligand complexes could be assumed as completely nonfluorescent. Except for the uncertain DAP-AT data, the errors in the binding parameters from fluorescence were estimated to be about the same as those of the absorbance titrations. For the polynucleotides, it was found relevant to use the McGhee–von Hippel binding model<sup>16,17</sup> (Table 2; Supporting Information, Figure B).

#### Effect of Salt Concentration on Binding Constants.

Absorption spectra in the region of 300–600 nm were recorded at several different ionic strengths for each diazapyrene. The fractions of free and bound ligand were determined by least-squares fitting of each spectrum to the spectra of free and bound ligand at 10 mM NaCl. By assuming that the number of binding sites was unaffected by the ionic strength, the binding constant  $K$  could be calculated. According to counterion condensation theory,  $\log K$  versus  $\log c_{\text{NaCl}}$  should give a linear plot with the slope proportional to the number of  $\text{Na}^+$  ions released per bound ligand molecule.<sup>18–22</sup> MDAP exhibits a slope of nearly  $-1$  (Figure 5), while DAP has a slope of only  $-0.4$ . The corresponding plot for DMDAP is markedly curved, the slopes in the high- and low-ionic-strength regions being approximately  $-1.4$  and  $-1.7$ , respectively.

When DAP binds to DNA at low ionic strength (1 mM NaCl), a new absorption band emerges at 413 nm. It decreases in intensity with increasing salt concentration, disappearing completely at 10 mM NaCl. The band was identified as HDAP<sup>+</sup>, the inadvertent protonation being attributed to trace of acid and poor buffer capacity of the low-ionic-strength solutions.

**Linear Dichroism.** Linear dichroism spectra were recorded for varied concentrations at a fixed phosphate/ligand (P/L) ratio of *ca.* 20 for MDAP and DMDAP and *ca.* 100 for DAP. No dependence of the spectral features on the total concentration of DNA and ligand could be seen. Both the  $L_a$  and  $L_b$  absorption bands show negative LD (Figure 6) in qualitative agreement with intercalation.<sup>12</sup> The negative LD excludes minor-groove binding which would have given positive LD for at least one of the  $L_a$  and  $L_b$  transitions.<sup>12</sup> The flow LD spectra of the three diazapyrenes in the presence of duplex poly(dA-

**Table 1.** Binding Constants and Site Densities for Diazapyrene–DNA Complexes<sup>a</sup>

DNA complex	$n$ (sites per base)	$K$ ( $\text{M}^{-1}$ )
DAP	$0.09 \pm 0.03$	$(1.3 \times 10^5) \pm 10^5$
MDAP	$0.17 \pm 0.03$	$(3.2 \times 10^5) \pm 10^5$
DMDAP	$0.15 \pm 0.03$	$(1.9 \times 10^5) \pm 10^5$

<sup>a</sup> According to eq 3.

**Table 2.** Binding Constants and Site Widths for Diazapyrenium–Polynucleotide Complexes<sup>a</sup>

complex	$K$ [ $\text{M bp}^{-1}$ ]	site width (bp)
DAP–GC <sup>b</sup>	$(8 \times 10^4) \pm 10^4$	$2.1 \pm 0.1$
MDAP–GC <sup>b</sup>	$(2 \times 10^6) \pm 10^5$	$1.3 \pm 0.2$
MDAP–AT <sup>b</sup>	$(2 \times 10^5) \pm 10^5$	$2.7 \pm 0.2$
DMDAP–GC <sup>b</sup>	$(8 \times 10^6) \pm 10^6$	$1.7 \pm 0.1$
DMDAP–AT <sup>b</sup>	$(2 \times 10^5) \pm 10^5$	$2.8 \pm 0.4$

<sup>a</sup> McGhee–von Hippel analysis of fluorescence titrations. <sup>b</sup> Non-cooperative model.

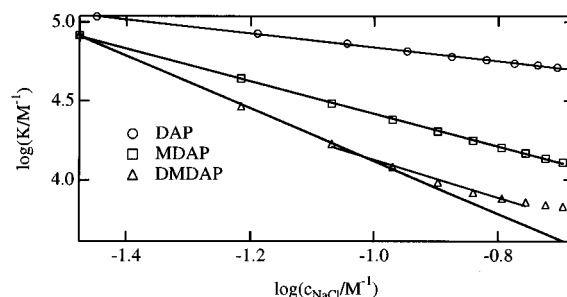


**Figure 5.** Salt dependencies of equilibrium constants. Plot of  $\log K$  versus  $\log c_{\text{NaCl}}$  with fitted lines.

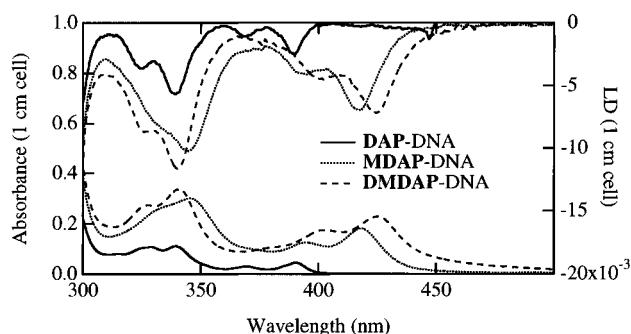


**Figure 6.** Linear dichroism (top) and absorption (bottom) of DAP (solid), MDAP (dotted), and DMDAP (dashed) bound to DNA.

dT) and poly(dG-dC) also show negative LD for all transitions (Figure 7a,b), although as a result of the poor orientation of the short polymers, the LD signals are much smaller and therefore more uncertain than for the diazapyrene–DNA complexes.

The reduced linear dichroism ( $\text{LD}^r = \text{LD}/A_{\text{iso}}$ ) provides information about the average orientations of the diazapyrene  $L_a$  and  $L_b$  transition moments relative to the DNA base transitions. Similar negative  $\text{LD}^r$  values are found for the DNA absorption (260 nm), the  $L_a$  region (300–350 nm), and the  $L_b$  region (360–450 nm), supporting that all transition moments are effectively perpendicular to the DNA helix axis (Table 3).<sup>12</sup>

An unexpected feature of  $\text{LD}^r$  is a pronounced variation over the absorption bands (Table 3; Figure 7c–h). Typically,  $\text{LD}^r$  spectra are structureless, except in regions of overlap between transitions of different polarizations. The observed spectral structure could in principle result from a heterogeneous binding distribution, e.g. both external binding and intercalation. Speaking against a two-site explanation, however, are the indifference of the LD and CD spectra (see below) to the P/L ratio and the presence of several distinct isosbestic points in the absorbance titrations.

(14) Pauluhn, J.; Zimmermann, H. W. *Ber. Bunsen-Ges. Phys. Chem.* **1978**, *82*, 1265–1278.

(15) Zimmermann, H. W. *Angew. Chem.* **1986**, *98*, 115–196.

(16) McGhee, J. D.; von Hippel, P. H. *J. Mol. Biol.* **1974**, *86*, 469–489.

(17) McGhee, J. D.; von Hippel, P. H. *J. Mol. Biol.* **1976**, *103*, 679.

(18) Friedman, R. A. G.; Manning, G. S.; Shahin, M. A. *The Polyelectrolyte Correction to Site Exclusion Numbers in Drug-DNA Binding*; Kallenbach, N. R., Ed.; Adenine Press: Schenectady, NY, 1988; pp 37–65.

(19) Bustamante, C.; Stigter, D. *Biopolymers* **1984**, *23*, 629–645.

(20) Record, M. T., Jr.; Woodbury, C. P.; Lohman, T. M. *Biopolymers* **1976**, *15*, 893–915.

(21) Wilson, W. D.; Lopp, I. G. *Biopolymers* **1979**, *18*, 3025–3041.

(22) Hopkins, H. P.; Wilson, W. D. *Biopolymers* **1987**, *26*, 1347–1355.

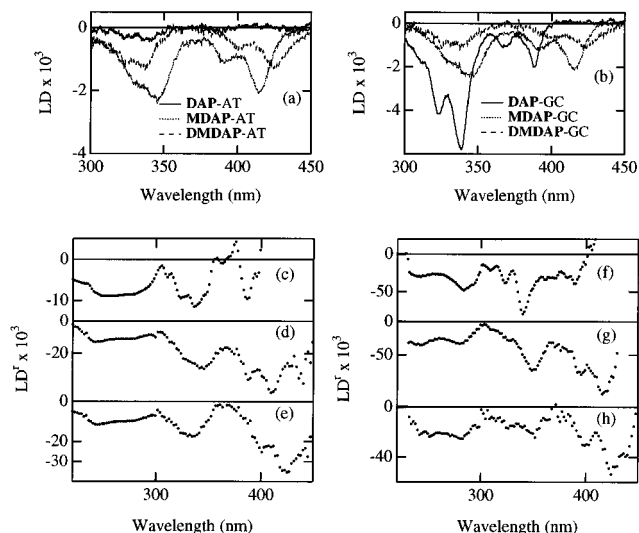


**Figure 7.** Linear dichroism of diazapyrenes bound to (a) poly(dA-dT)<sub>2</sub> and (b) poly(dG-dC)<sub>2</sub> and (c–h) reduced linear dichroism for (c) DAP–AT, (d) MDAP–GC, (e) DMDAP–AT, (f) DAP–GC, (g) MDAP–GC, and (h) DMDAP–GC. Note the variations in LD' over each electronic transition ( $L_a$ : 300–350 nm;  $L_b$ , 380–450 nm) for all diazapyrene–polynucleotide complexes.

**Table 3.** Reduced Linear Dichroism (LD') for the Diazapyrene–DNA Complexes<sup>a</sup>

DNA complex	LD' (DNA)	LD' ( $L_a$ )			LD' ( $L_b$ )		
DAP	-0.033	-0.024	-0.020	-0.035	-0.025	-0.014	-0.048
MDAP	-0.033	-0.032	-0.032	-0.034	-0.033	-0.032	-0.041
DMDAP	-0.033	-0.032	-0.035	-0.035	-0.026	-0.025	-0.031

<sup>a</sup> The three values for each transition refer to, respectively, the first vibronic peak, the trough between the first two peaks, and the second vibronic peak (cf. Figure 6).

**Circular Dichroism.** For a number of DNA-binding molecules several binding modes are known to occur in parallel. To investigate this point, induced CD spectra for DMDAP–DNA and MDAP–DNA were recorded. The ligands are achiral themselves, but as a result of interaction with the chiral DNA, they acquire a rotational strength, whose sign and magnitude depends on the binding geometry: ligand–ligand stacking expected to give strong bisignate exciton CD, while intercalation should give weak induced CD.<sup>23–25</sup> For the cations MDAP and DMDAP, a negative CD band is observed in the  $L_b$  absorption region and a positive one for the  $L_a$  band (Supporting Information, Figure B), both being weak as expected for intercalators.<sup>24</sup> No significant changes in the CD spectral features were found when the P/L ratio was changed between 10 and 30 (Supporting Information, Figure D).

**Fluorescence.** The fluorescence of MDAP and DMDAP is completely quenched by DNA and by the AT and GC polynucleotides. DAP is quenched by GC but forms a fluorescent complex with AT. Lifetime measurements on the latter show the formation of a longer-lived species ( $\tau = 24$  ns ( $\chi^2 = 1.3$ ); DAP,  $\tau = 14.4$  ns ( $\chi^2 = 1.1$ )).

**Thermodynamics.** Thermodynamic parameters of binding of DAP, MDAP, and DMDAP to CT DNA were evaluated from van't Hoff plots of the macroscopic equilibrium constants (Figure 8; Table 4). Reaction enthalpies for MDAP–DNA and DMDAP–DNA were also measured calorimetrically (Figure 9), DAP being too insoluble for calorimetric measurements.

(23) Nordén, B.; Tjerneld, F. *Biopolymers* **1982**, *21*, 1713–1734.

(24) Lyng, R.; Rodger, A.; Nordén, B. *Biopolymers* **1991**, *31*, 1709–1820.

(25) Schipper, P. E.; Nordén, B.; Tjerneld, F. *Chem. Phys. Lett.* **1980**, *70*, 17–21.

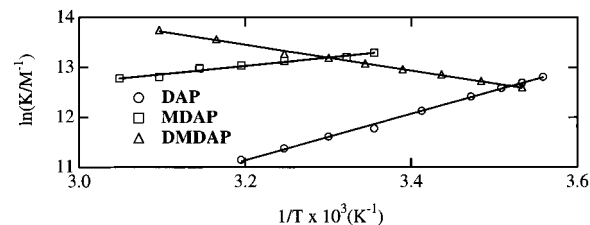


**Figure 8.** Evaluation of thermodynamic parameters from equilibrium data. van't Hoff plots for DAP–DNA, MDAP–DNA, and DMDAP–DNA. Ligand and concentrations were chosen to correspond approximately to 50% bound ligand (DAP:DNA, 30:600  $\mu$ M; MDAP:DNA, 30:210  $\mu$ M; DMDAP:DNA, 30:120  $\mu$ M).

**Table 4.** Thermodynamic Quantities for the Diazapyrene–DNA Complexes

DNA complex	$\Delta G^\circ$ <sup>a</sup>	$\Delta G_{pc}$ <sup>a</sup>	$\Delta G_t$ <sup>a</sup>	$\Delta H_{obs}$ <sup>a</sup>	$\Delta S_{obs}$ <sup>b</sup>	$\Delta S_{Na^+}$ <sup>b</sup>	$\Delta S_0$ <sup>b,c</sup>
DAP <sup>d</sup>	-6.9	-1.1	-5.8	-9.0	-7	+4	-11
DAP <sup>e</sup>				nd <sup>f</sup>	nd		
MDAP <sup>d</sup>	-7.4	-2.7	-4.7	-3.3	+15	+9	+6
MDAP <sup>e</sup>				-3.0	+12		
DMDAP <sup>d</sup>	-7.1	ca. -5	ca. -2	+5.2	+43	+16	+27
DMDAP <sup>e</sup>				bc <sup>g</sup>			

<sup>a</sup> In kcal/mol. <sup>b</sup> In cal/(mol K). <sup>c</sup> Calculated as  $\Delta S_0 = \Delta S_{obs} - \Delta S_{Na^+}$ , see text (Discussion). <sup>d</sup> From van't Hoff plot. <sup>e</sup> Calorimetrically. <sup>f</sup> nd = not determined. <sup>g</sup> bc = biphasic curve, see text (Discussion).

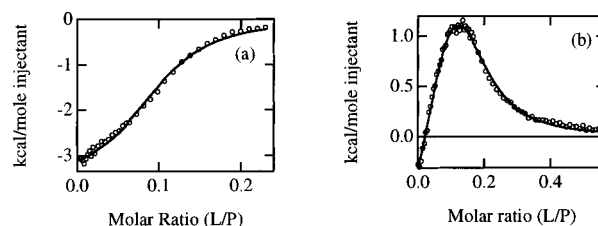


**Figure 9.** Binding isotherms obtained from calorimetric measurements at 27 °C (heat evolved per mole of injectant vs ligand:DNA ratio): (a) MDAP (ca. 3 mM) titrated into DNA (ca. 0.8 mM bases), and (b) DMDAP (ca. 4 mM) titrated into DNA (ca. 1 mM bases). Solid lines are best fits to (a) a single-site model and (b) a two-independent-sites model.

For MDAP, a single-site analysis (Figure 9a) yields the same  $\Delta H$  and  $\Delta S$  results as those obtained from the spectroscopic data, whereas for DMDAP, a biphasic reaction heat isotherm (Figure 9b) contrasts the spectroscopic titration and indicates the involvement of a second binding site. Discrepancy between directly measured enthalpy and enthalpy calculated from a van't Hoff plot could arise as the result of a change in heat capacity, which will result in curved van't Hoff plots.<sup>26</sup> However, the calorimetrically measured enthalpies appear to be temperature-independent (17 and 27 °C) and the van't Hoff plots linear, so this effect does not apply here.

## Discussion

**Electronic Spectra.** The spectral features of all three diazapyrenes are strongly influenced by their interactions with DNA. The presence of several distinct isosbestic points in the absorbance titrations with DNA shows that they can be described in terms of two spectroscopically distinguishable species: free and bound. The probability that two bound forms would have identical absorption spectra over a wide wavelength range must be regarded as small, particularly in view of the sensitivity toward the environment of the diazapyrene chromophore. Thus, for example, intercalation and groove binding modes should have distinctly different spectra. Even minor spectral differ-

(26) Naghibi, H.; Tamura, A.; Sturtevant, J. M. *Proc. Natl. Acad. Sci. U.S.A.* **1995**, *92*, 5597–5599.

ences, such as those between a free and an externally bound ligand, are anticipated to blur the isobestic points and impair the fitness of the spectral binding analysis.

**Binding Properties.** The binding of DAP, MDAP, and DMDAP to polynucleotides AT and GC was expected to be homogeneous enough to justify a McGhee–von Hippel analysis.<sup>16</sup> The results for DMDAP are within experimental error in agreement with previous measurements using fluorescence quenching.<sup>8,9</sup>

The binding to GC of MDAP appears to approach a 1:1 ligand:base-pair stoichiometry rather than the 1:2 nearest-neighbor exclusion mode found for the DAP and DMDAP GC complexes. It is conceivable that partial neutralization of the cationic charge of MDAP by charge-transfer interaction with one of the purine nucleobases could account for a higher stoichiometry, while phosphate electrostatic interactions should probably not be overestimated.<sup>27</sup> The smaller binding constant for MDAP–AT compared to MDAP–GC may be attributed to reduced charge-transfer interaction between MDAP and adenosine. We also found the fluorescence of MDAP and DMDAP to be quenched efficiently by millimolar concentrations of the purine mononucleotides dA and dG but not by the pyrimidine nucleotides dT and dC. This leads us to conclude that charge-transfer and supporting hydrophobic interactions of MDAP and DMDAP are more pronounced with the purine than with the pyrimidine nucleobases.

The biphasic binding isotherm for DMDAP–DNA obtained from calorimetric measurements is showing both an exothermic (high P/L) and an endothermic (low P/L) region (Figure 9b). We have at present no satisfactory explanation for this observation.

**LD and Induced CD.** The energetically well separated  $L_a$  and  $L_b$  transitions of the diazapyrenes should be ideal for determining binding geometries from LD spectra, except that the observed structured  $LD^f$  complicates interpretation. Variations of  $LD^f$  could be due to the following: (1) *Free ligand* would distort the  $A_{iso}$  spectrum and as only bound ligand contributes to the LD, the  $LD^f$  calculated as  $LD/A_{iso}$  would vary with wavelength. Due to the sharp absorption peaks of the free diazapyrenes, even small amounts of free ligand might significantly distort the  $LD^f$ . (2) *Heterogeneous binding*, such as both intercalation and groove binding or external binding, would provide different orientations of the transition moments and environmental energy shifts. (3) Binding by intercalation could be macroscopically homogeneous but still *microscopically heterogeneous* if the ligand displays lateral mobility (partial intercalation) or rotation in the intercalation pocket.

To discriminate between these possibilities, the following controls were made: (i) Subtracting from  $A_{iso}$  a small fraction of the absorption spectrum of free ligand did not remove the structure of the calculated  $LD^f$ . Free ligand is therefore excluded as a main source of the variations. (ii) LD spectra were recorded at a series of P/L ratios from 5 to 100. If binding modes with different binding geometries had been populated with increasing binding ratio, the shape of the LD spectrum would have been P/L-dependent. However, all LD spectra could be linearly combined to yield a zero LD over the whole ligand absorption range of 300–500 nm, i.e. their shape was independent of P/L. Likewise, the CD spectra of DMDAP–DNA and MDAP–DNA were found to be independent of the P/L ratio. The presence of both external and intercalative binding modes for DMDAP has been proposed previously.<sup>8</sup> Our results, however, suggest only one type of bound species. (iii) The diazapyrenes bound to AT and GC showed, albeit less pronounced, the same

characteristic structure in  $LD^f$  as the complexes with DNA. We therefore rule out sequence heterogeneity as a main source of the  $LD^f$  variations.

The remaining explanation for the observed structured  $LD^f$  spectrum is a microscopic heterogeneity due to rotation of the ligand within a tilted intercalation pocket or a lateral movement between full and partial intercalation. Various studies indicate that the nucleobases of B-DNA may be inclined as much as 20° from perpendicularity.<sup>12,28,29</sup> If the spectral shift of the ligand depends on how it is rotated in the intercalation pocket, a rotational distribution in a tilted pocket would explain the structured  $LD^f$ .

A precise assessment of the binding geometries is difficult solely from the spectroscopic data. However, using the base-pair tilt, we may distinguish between an arrangement where the diazapyrene long axis is parallel to the (inclined) base-pair long axis or parallel to the (perpendicular) base-pair short axis. In the former case, the diazapyrene  $L_b$  transition (short axis) will be at a *larger angle* to the helix axis and, thus, the  $LD^f$  of the  $L_b$  transition will be *more negative* than that of the  $L_a$  transition. The latter case will give a more negative  $LD^f$  for  $L_a$  than for  $L_b$ . From the  $LD^f$  of the diazapyrene–polynucleotide complexes (Figure 7c–h), we conclude that MDAP and DMDAP both tend to bind with their long axes parallel to the base-pair long axis, while DAP binds rather with its long axis perpendicular to the base-pair long axis.

The induced CD spectra support the notion that the cations MDAP and DMDAP bind in a similar fashion, while the neutral DAP binds in a different way. According to experiments and theoretical studies an intercalated chromophore centered near the helix axis of DNA should exhibit negative induced CD for all long-wavelength transitions polarized parallel to the long axis of the base-pair pocket, while transitions perpendicular to this direction, but still in the plane of the nucleobases (i.e., parallel to the pseudo-dyad axis), should give positive CD.<sup>23–25</sup> The CD spectra thus suggest that MDAP and DMDAP bind with their long axes parallel to the base-pair long axis (negative induced CD for the  $L_a$  and positive for the  $L_b$  transition).

**Thermodynamics and Salt Effects.** When passing from the electrically neutral DAP to the dication DMDAP, the driving force for intercalation clearly goes from enthalpy to entropy. The binding of DAP to DNA involves a large negative  $\Delta S^\circ$ , contrary to what one may expect when considering release of the DAP water shell in the reaction  $DAP(aq) \rightarrow DAP-DNA$ .<sup>30–34</sup> We believe the binding thermodynamics reflects a subtle balance between electrostatic forces (hydrogen bonds and multipole interactions) and entropic effects. The change in entropy is governed by release of counterions and water from DNA as well as ligand but also changes in the local DNA structure upon binding of the ligand may be important.

For the transfer of *small* molecules from polar to nonpolar environments, hydrophobic interactions give  $\Delta H > 0$  and  $\Delta S > 0$  accompanied by a negative  $\Delta C_p$ . The enthalpic loss in the transfer is due to the fact that interwater hydrogen bonds around a *small* hydrophobic molecule are *stronger* than those in the bulk solution. Since the hydration shell is more restricted than the bulk water,  $\Delta S$  for this process is  $> 0$ . For *large* molecules,

(28) Lincoln, P.; Broo, A.; Nordén, B. *J. Am. Chem. Soc.* **1996**, *118*, 2644–2653.

(29) Kang, H.; Johnson, C. W. *Biopolymers* **1993**, *33*, 245–253.

(30) Ben-Naim, A. *Hydrophobic Interactions*; Plenum Press: New York, 1980.

(31) Miller, J. L.; Kollman, P. A. *J. Phys. Chem.* **1996**, *100*, 8587–8594.

(32) Ha, J.-H.; Spolar, R. S.; Record, M. T. *J. Mol. Biol.* **1989**, *209*, 801–816.

(33) Sturtevant, J. M. *Proc. Natl. Acad. Sci. U.S.A.* **1977**, *76*, 2236–2240.

(34) Grunwald, E.; Steel, C. *J. Am. Chem. Soc.* **1995**, *117*, 5687–5692.

(27) Misra, V. K.; Honig, B. *Proc. Natl. Acad. Sci. U.S.A.* **1995**, *92*, 4691–4695.

however,  $\Delta H$  for the transfer is *negative*, due to the disruption of hydrogen bonds in the formation of the cavity for the solute.  $\Delta S$  should still be positive.

If we consider DAP a “large” molecule and assume that intercalation involves favorable electrostatic interactions, we can explain the large negative  $\Delta H$ . The energy of a hydrogen bond in water is about 5 kcal/mol,<sup>35</sup> so the binding enthalpy of DAP could, for example, be accounted for by one hydrogen bond assisted by attractive electrostatic interactions with the nucleobases. We have no satisfactory explanation of the negative  $\Delta S^\circ$  other than that the classical hydrophobic effect in this case is masked by a decreased entropy of the ligand–DNA complex, e.g. due to the restricted mobility.

Although cationic intercalators generally seem to bind exothermally,<sup>22,36–38</sup> the observation that the heat of binding for the cationic MDAP is smaller than for the neutral DAP is not surprising, in view of that adding one positive charge to the diazapyrene skeleton will reduce the hydrophobic surface of the molecule, leading to a less negative  $\Delta H_{\text{hydrophobic}}$ . Furthermore, when MDAP binds to DNA, coordinated anions and water will be released from the hydrophilic pyridinium nitrogen,<sup>39</sup> a process expected to give positive  $\Delta H$  and  $\Delta S$  contributions. In addition, MDAP has lost one of the two possible hydrogen-bonding pyridine sites of DAP that could contribute to the negative  $\Delta H$  of the latter ligand.

The arguments outlined for MDAP also apply to DMDAP. Furthermore, DMDAP must place at least one of its two positive charges<sup>40</sup> inside the DNA helix when it intercalates, which is most probably energetically unfavorable and thus further increases  $\Delta H$ . From Table 4 it is clear that the release of electrostricted water and counterions from the charged ligands (MDAP and DMDAP) forms a large contribution to the thermodynamic behavior of the DNA complexes, by simultaneously giving unfavorable  $\Delta H$  and favorable  $\Delta S$  contributions to the binding free energy.

According to counterion condensation theory, the parameter  $s$ , defined as  $\partial(\ln K_{\text{obs}})/\partial(\ln [\text{salt}])$ , is a measure of the number of sodium ions released from DNA per bound ligand.<sup>18–20,41–46</sup> Due to the lengthening of the DNA helix upon intercalation, even non-ionic intercalators show a salt dependence of the binding constant. The results for the diazapyrenes are in agreement with theory and for DAP supports our other evidence for intercalation, since if it had been bound externally,  $s$  would have been expected to be zero.

It has been argued that the total free energy of binding should be partitioned into “nonelectrostatic” and “polyelectrolyte”

(35) Feyereisen, M. W.; Feller, D.; Dixon, D. A. *J. Phys. Chem.* **1996**, *100*, 2993–2997.

(36) Kagemoto, A.; Yoshii, A.; Kimura, S.; Baba, Y. *J. Phys. Chem.* **1994**, *98*, 5943–5952.

(37) Kagemoto, A.; Kunihiro, A.; Baba, Y. *Thermochim. Acta* **1994**, *242*, 65–75.

(38) Baba, Y.; Kunihiro, A.; Kagemoto, A. *Thermochim. Acta* **1992**, *202*, 241–248.

(39) Collins, K. D. *Proc. Natl. Acad. Sci. U.S.A.* **1995**, *92*, 5553–5557.

(40) Ab initio calculations at the HF/6-31G\*/PM3 level (results not shown) indicate that 60–70% of the positive charge is localized around the nitrogens.

(41) Friedman, R. A. G.; Manning, G. S. *Biopolymers* **1984**, *23*, 2671–2714.

(42) Hagmar, P.; Pierrou, S.; Nielsen, P.; Nordén, B.; Kubista, M. *J. Biomol. Struct., Dyn.* **1992**, *9*, 667–679.

(43) Chaires, J. B.; Priebe, W.; Graves, D. E.; Burke, T. G. *J. Am. Chem. Soc.* **1993**, *115*, 5360–5364.

(44) Chaires, J. B.; Satyanarayana, S.; Suh, D.; Fokt, I.; Przewlaka, T.; Priebe, W. *Biochemistry* **1996**, *35*, 2047–2053.

(45) Wilson, W. D.; Tanius, F. A.; Watson, R. A.; Barton, H. J.; Strekowska, A.; Harden, D. B.; Strekowski, L. *Biochemistry* **1989**, *28*, 1984–1992.

(46) Loontjens, F. G.; Regenfuss, P.; Zechel, A.; Dumortier, L.; Clegg, R. M. *Biochemistry* **1990**, *29*, 9029–9039.

components with the latter given as<sup>43,44</sup>

$$\Delta G_{\text{pe}} = sRT \ln [\text{Na}^+] \quad (4)$$

The difference between  $\Delta G^\circ$  and  $\Delta G_{\text{pe}}$  is the salt-independent, “nonelectrostatic” portion ( $\Delta G_{\text{t}}$ ) of the binding free energy. The shift in driving force from enthalpy to entropy is paralleled by a more negative  $\Delta G_{\text{pe}}$ . Since  $\Delta G^\circ$  is approximately the same for all the diazapyrene–DNA complexes, we conclude that the contribution of  $\Delta G_{\text{t}}$  to the binding decreases in the series DAP > MDAP > DMDAP. This supports the notion that hydrophobicity and electrostatic interactions complement each other in the binding to DNA.

Correspondingly, we could estimate the contribution to  $\Delta S$  from the release of counterions according to<sup>21,22</sup>

$$\Delta S_{\text{Na}^+} = -\{m'\psi^* + 2N(\psi - \psi^*)\}R \ln [\text{Na}^+] \quad (5)$$

where the factor  $-\{m'\psi^* + 2N(\psi - \psi^*)\}$  is equal to  $s$ .<sup>21</sup> The calculated  $\Delta S_{\text{Na}^+}$  values at 10 mM NaCl are found in Table 4. Since the non-polyelectrolyte contribution  $\Delta S_0$  increases from  $-11$  cal/(mol K) for DAP–DNA to  $+6$  cal/(mol K) for MDAP–DNA and to  $+27$  cal/(mol K) for DMDAP–DNA, it is clear that other factors than the polyelectrolyte effect strongly influence the binding entropy.

## Conclusions

(1) Diazapyrenes DAP, MDAP, and DMDAP bind by intercalation or partial intercalation between DNA base pairs, as judged from strong interactions with the nucleobases in conjunction with approximately perpendicular orientations of the molecular planes relative to the DNA helix axis. The signs of the induced circular dichroism bands of the diazapyrene chromophore, together with the fact that the  $\text{LD}^{\text{r}}$  in the  $\text{L}_b$  band is more negative than the  $\text{LD}^{\text{r}}$  of the DNA bases, suggest that the long axes of MDAP and DMDAP are preferentially oriented parallel to the longest dimension of the base-pair intercalation pocket.

(2) A pronounced fine structure of the reduced linear dichroism spectra suggests that the diazapyrenes have considerable motional freedom in an intercalation pocket that is tilted from perpendicularity to the DNA helix axis. The decrease in fine structure for the series DAP > MDAP > DMDAP suggests that ionic charge significantly reduces this ligand mobility.

(3) The binding thermodynamics can be interpreted in terms of a balance between hydrophobic and electrostatic interactions. In the series DAP, MDAP, DMDAP, the driving force of binding is shifted from enthalpy to entropy as the character of the ligand is gradually shifted from hydrophobic to hydrophilic. The release of counterions from DNA is only a minor contribution to  $\Delta S^\circ$ , while the release of electrostricted water from the ionic ligands MDAP and DMDAP influences the thermodynamic parameters strongly. Another factor that may contribute to the binding entropy is distortion of the DNA structure.

**Acknowledgment.** This project is supported by the Swedish Natural Science Research Council.

**Supporting Information Available:** Fluorescence titration of MDAP with GC, McGhee–von Hippel plots for DAP–GC, MDAP–GC, MDAP–AT, DMDAP–GC, and DMDAP–AT, CD spectra of MDAP–DNA and DMDAP–DNA at different P/L ratios, and CD spectra of DAP–DNA, MDAP–DNA, and DMDAP–DNA (2 pages). See any current masthead page for ordering and Internet access instructions.